BULLETIN OF THE POLISH ACADEMY OF SCIENCES
TECHNICAL SCIENCES, Vol. 67, No. 1, 2019
DOI: 10.24425/bpas.2018.126120

Fractional-order feedback control of a pneumatic servo-drive

P.A. LASKI*

Kielce University of Technology, Department of Automation and Robotics, Faculty of Mechatronics and Machine Design,
Aleja Tysiaclecia Panstwa Polskiego 7, 25-314 Kielce, Poland

Abstract. A fractional-order control strategy for a pneumatic position servo-system is presented in this paper. The idea of the fractional calculus application to control theory was introduced in many works, and its advantages were proved. This paper deals with the design of fractional order $PI^{\lambda}D^{\mu}$ controllers, in which the orders of the integral and derivative parts, λ and μ, respectively, are fractional. Experiments with fractional-order controller are performed under various conditions, which include position signal with different frequencies and amplitudes or a step position signal. The results show the effectiveness of the proposed schemes and verify their fine control performance for a pneumatic position servo-system.

Key words: pneumatic servo-drive, fractional-order, identification and control.

1. Introduction

Pneumatic drives are still used frequently in automation and constitute a base for performing simple movements used for changing plants' orientation and for translation on automated production lines. They have many positive features, including high durability, simple construction, operation reliability, ability to work in a highly polluted and dusty environment (also in explosion risk areas) and high overload capacity. Additionally, the operating medium used in the drive is widely available. However, precise control of a pneumatic drive proves very difficult, because of high compressibility of air. In practice, it only allows the pneumatic drive to be put in extreme positions, which are set mechanically. Furthermore, nowadays pneumatic drives and their control systems are expected to meet increasingly strict requirements. Meanwhile, controlling and positioning of pneumatic drives, due to their widespread use, are still tangible subjects for researchers at many research centers around the world.

Although pneumatic drives have been known for many decades, new papers are still being reported. They present solutions for theoretical models that focus on drives dynamics [1, 2] tracking positioning [3], friction in insulating nodes [4, 5], innovative control valves [6, 7], flexible muscle [8–10] drives or heat transfer of the operating medium [11] as well as modeling of the medium flow [12]. Positional and follow-up control of pneumatic drives are complicated issues and require use of modern valves with high dynamics and taking innovative approaches to applying algorithms and controllers. Both experimental and simulated results of research work on positioning of pneumatic drives highlight the need for using a new type of control system. For that reason, attempts have been made to use fractional order controllers to improve the quality of positional and follow-up control of the pneumatic drive. This subject is presented in this article.

2. Dynamic model of a pneumatic servo-drive

2.1. Test stand for pneumatic drive. To evaluate dynamic properties of a pneumatic drive, the test stand shown in Fig. 1 was made. The stand consists of a single rodless cylinder by Norgren with a piston 32 mm in diameter and a nominal length of 0.6 m. The actuator has side-sliding guides. To determine the position of the piston, the actuator is equipped with a non-contact magnetic position external sensor.

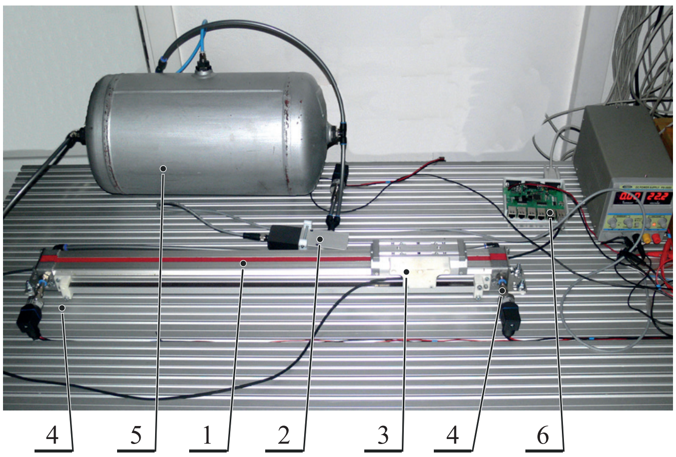

Fig. 1. Test stand for pneumatic drive: 1 – rodless cylinder, 2 – directional control valve, 3 – displacement transducer, 4 – pressure transducers, 5 – pneumatic power supply, 6 – measurement data acquisition system

*e-mail: pawell@tu.kielce.pl

Manuscript submitted 2018-01-26, revised 2018-11-19, initially accepted for publication 2018-12-14, published in February 2019.

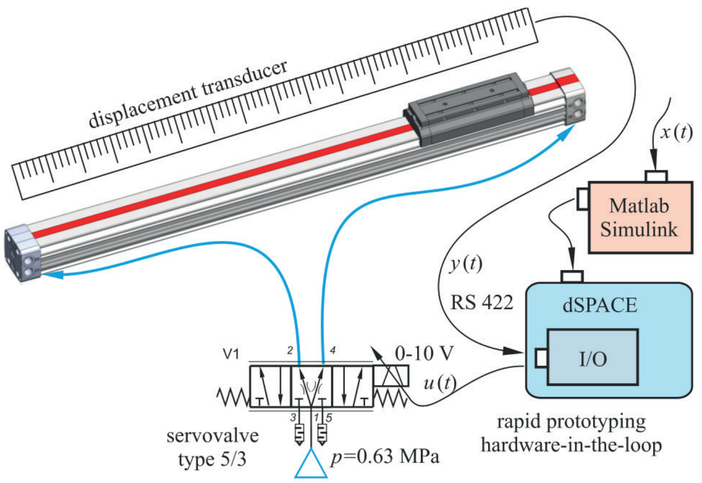

Fig. 2. Schematic diagram of pneumatic servo-drive

The sensor has 0.01 mm measuring accuracy within the whole length range. The weight of the cylinder piston with load equals 0.8 kg. To eliminate the influence of "sticking friction" of the test actuator, the test was done within the nominal length range between 0.1 m and 0.5 m. The control actuator is equipped with a proportional flow MPYE-5–1/8-HF-010 valve, type 5/3, by Festo. Minimum response time of the valve is 14 ms while supply pressure equals 0.63 MPa. The valve is controlled by voltage in the range of 0–10 V, and the value of 5 V corresponds to the central position of the valve, where constant and equal value of pressure is set on 2 and 5 working paths.

2.2. Pneumatic servo-drive identification. Due to the fact that the plant is identified by a system consisting of the pneumatic actuator, which is controlled by proportional directional control valves, the negative feedback loop and proportional gain method was used. The pneumatic drive is characterized by high variability of friction forces, especially in first operation cycles after longer periods of non-usage. A research experiment was therefore planned and consisted of dozens of adjustable actuator movements with randomly generated positions. Only after that were proper tests conducted. During those tests, the response to step function was obtained corresponding to move work from point to point of the actuator. In the identification process, the excitation signal was the valve controlling signal and response was measured by the actuator position.

2.3. Pneumatic servo-drive identification using classic transfer function. Based on the research conducted and following an identification process, two mathematical models for describing the pneumatic servo-drive were proposed. The first model would use the classic equivalent transfer function, while the second one was obtained by using the fractional order model.

In the identification model process of the pneumatic servo-drive plant, the Matlab identification toolbox was used. This paper proposed a plant described by transfer function of third order. Within the identification process, the plant fit estimation data at the level of 93.05% were found. Thus, the form of the plant equivalent transfer function is presented by the following equation:

$$G(s)_{ob} = \frac{K_{p1}}{\left(1 + 2\zeta T_w s + (T_w s)^2\right)\left(1 + T_p s\right)} \tag{1}$$

where:

$T_w = 0.045$,
$K_{p1} = 1.0034$,
$\zeta = 0.6082$,
$T_p = 0.0542$,

which, after inserting, gave:

$$G(s)_{ob} = \frac{1}{(1 + 0.0542s)} \cdot \frac{1.0034}{\left(1 + 0.0548s + (0.045s)^2\right)}. \tag{2}$$

A frequency identification process using Fourier transform from the Wolfram Mathematica program was also performed.

Therefore, when identifying parameters of the pneumatic servo-model, the whole process was based on the fact that the actual signal is given by a periodic signal and the response is recorded in steady-state conditions for a closed system (Fig. 3, Fig. 4).

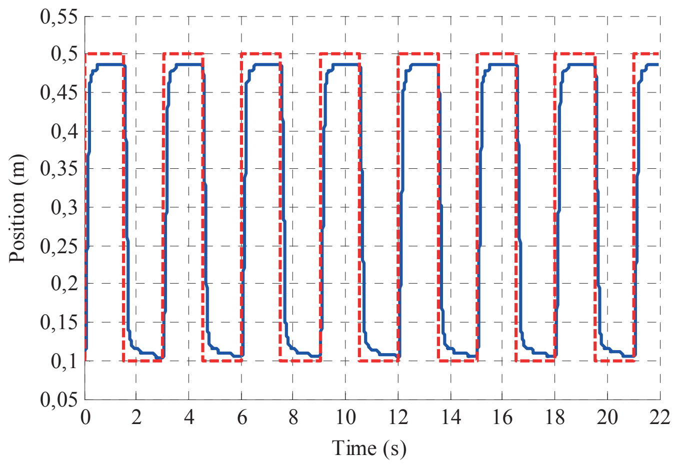

Fig. 3. Plant's response to periodic signal

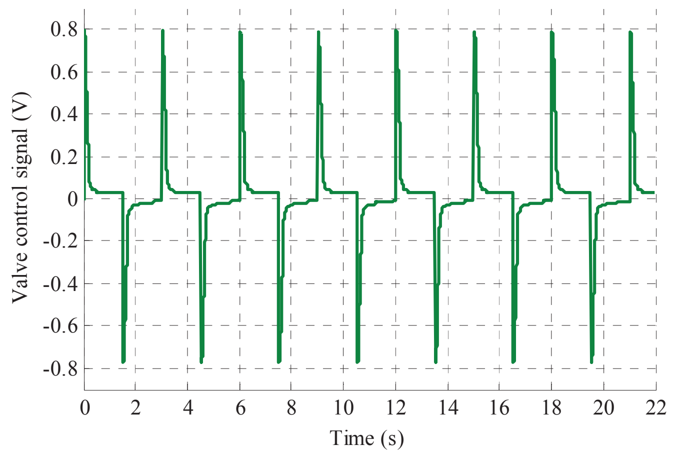

Fig. 4. Valve control signal

This allowed for model identification based on the input and output spectrum signals.

The identification process relied on determining the rising edges' location of a set signal and determining the beginning and ending samples' indices of the course test, the number of samples and the number of waves. Next, the Fourier transform (DFT) was determined for the analyzed course.

In the periodic function, for which the exact course of M function periods is recorded, only every M component is non-zero. In the analyzed case, those will be $2M$ signal course periods, because the wave is odd and has the character of a rectangular waveform. The indices of non-zero value of harmonic components are calculated next. Parameters of the servo-drive plant model were determined by means of the optimization method. Because the plant's response to an input signal with a harmonic component U_k is equal to:

$$Y_k = H(j\omega_k)U_k \tag{3}$$

it was assumed that the minimized quality index will have the following form:

$$J = \sum_{k=1}^{m} \left| Y_{Mk} - H(j\omega_{Mk})U_{Mk} \right|^2 . \tag{4}$$

And so, in equation (4), the sum for the appropriate value m considers only the non-zero harmonics of the signals. Because the pneumatic cylinder is an integral-type plant, the transfer function model was assumed in the form of:

$$H(j\omega)_{ob} = \frac{K_{p2}}{s(T_1 s^2 + T_2 s + 1)} . \tag{5}$$

Coefficients of the transfer function model were obtained based on an objective function, for which value J takes the smallest value, thus:

$$H(j\omega)_{ob} = \frac{2.325}{\mathrm{s}(0.000725 s^2 + 0.02704 s + 1)} . \tag{6}$$

2.3. Pneumatic servo-drive identification as transfer function of fractional order. Fractional calculus is a generalization of integration and differentiation to a non-integer order operator, ${}_a\mathscr{D}_t^\alpha$, where a and t denote the limits of the operation and α denotes the fractional order so that:

$$ {}_a\mathscr{D}_t^\alpha = \begin{cases} \dfrac{\mathrm{d}^\alpha}{\mathrm{d}t^\alpha} & \Re(\alpha) > 0, \\ 1 & \Re(\alpha) = 0, \\ \displaystyle\int_a^t (\mathrm{d}\tau)^{-\alpha} & \Re(\alpha) < 0, \end{cases} \tag{7}$$

where: generally, it is assumed that $\alpha = \mathbb{R}$, but it may also be a complex number.

There exist multiple definitions of the fractional differintegral. The Riemann-Liouville differintegral is a commonly used definition.

Definition 1. (R–L definition)

$$ {}_a\mathscr{D}_t^\alpha f(t) = \frac{1}{\Gamma(m-\alpha)} \left(\frac{d}{\mathrm{d}t}\right)^m \int_a^t \frac{f^{(m)}(\tau)}{(t-\tau)^{\alpha-m+1}} \mathrm{d}\tau \tag{8}$$

where: $m - 1 < \alpha < m$, $m \in \mathbb{N}$, $\alpha \in \mathbb{N}^+$ and $\Gamma(\cdot)$ is Euler's gamma function.

The next definition relates to the fractional derivative as defined by Caputo [14].

Definition 2. (Caputo definition)

$$ {}_a\mathscr{D}_t^\alpha f(t) = \frac{1}{\Gamma(m-\alpha)} \int_0^t \frac{f(\tau)}{(t-\tau)^{\alpha-m+1}} \mathrm{d}\tau , \tag{9}$$

where $m - 1 < \alpha < m$, $m \in \mathbb{N}$.

Consider also the Grünwald-Letnikov definition.

Definition 3. (G–L definition)

$$ {}_a\mathscr{D}_t^\alpha f(t) = \lim_{h\to 0} \frac{1}{h^\alpha} \sum_{j=1}^{\left[\frac{t-a}{h}\right]} (-1)^j \binom{\alpha}{j} f(t-jh) \tag{10}$$

where: [.] means the integer part.

The Laplace transform is an essential tool in linear dynamic system modeling and control system engineering. Function $H(s)$ of the complex variable $s = \sigma + j\omega$ is called the Laplace transform of the original function $h(t)$, and is defined in the following manner:

$$H(s) = \mathcal{L}[h(t)] = \int_0^\infty e^{-st} h(t) \mathrm{d}t . \tag{11}$$

The original function $h(t)$ can be recovered from the Laplace transform by applying the reverse Laplace transform defined as:

$$h(t) = \mathcal{L}^{-1}[H(s)] = \frac{1}{2\pi j} \int_{c-j\infty}^{c+j\infty} e^{st} H(s) \mathrm{d}s \tag{12}$$

where c is greater than the real part of all the poles of function $H(s)$ [13, 14].

Assuming zero initial conditions, the Laplace transform of a generalized fractional-order operator is given by:

$$\mathcal{L}^{-1}[\mathscr{D}^\alpha h(t)] = s^\alpha H(s) . \tag{13}$$

It should be noted that if the initial conditions are not zero, different definitions apply for the Riemann-Liouville and Grünwald-Letnikov fractional-order operators.

2.3.1. Fractional-order models. A fractional-order continuous-time dynamic system can be expressed by a fractional differential equation of the following form:

$$\begin{aligned} & a_n \mathscr{D}^{\alpha_n} y(t) + a_{n-1} \mathscr{D}^{\alpha_{n-1}} y(t) + \dots + a_0 \mathscr{D}^{\alpha_0} y(t) = \\ & = b_m \mathscr{D}^{\beta_m} u(t) + b_{m-1} \mathscr{D}^{\beta_{m-1}} u(t) + \dots + b_0 \mathscr{D}^{\beta_0} u(t). \end{aligned} \tag{14}$$

The system is said to be of commensurate order if in (14) all the orders of derivation are integer multiples of a base order γ such that $\alpha_k, \beta_k = k\gamma, \gamma \in \mathbb{R}^+$ [15]. The system can then be expressed as:

$$\sum_{k=0}^{n} a_k \mathscr{D}^{k\gamma} y(t) = \sum_{k=0}^{m} b_k \mathscr{D}^{k\gamma} u(t). \tag{15}$$

Applying the Laplace transform to (14) with zero initial conditions the input-output representation of the fractional-order system can be obtained in the form of a transfer function:

$$G(s) = \frac{Y(s)}{U(s)} = \frac{b_m s^{\beta_m} + b_{m-1} s^{\beta_{m-1}} + \dots + b_0 s^{\beta_0}}{a_n s^{\alpha_n} + a_{n-1} s^{\alpha_{n-1}} + \dots + a_0 s^{\alpha_0}}. \tag{16}$$

In the pneumatic servo-drive plant identification process, the fractional-order Modelling and Control library was used. This toolbox is integrated with the Matlab program. Furthermore another, FOMCOM-based library provides time-domain and frequency-domain fractional-order system analysis along with verifying system stability [16, 17]. In the toolbox, fractional-order systems are given by fractional-order transfer function plants in the form of (14). These plants are generalizations of the rational transfer functions to the fractional order.

As previously, the plant was identified in the frequency domain by using the Fourier transform, but with the difference that the plant was described as a fractional order transfer function as follows:

$$H(s)_{FO} = \frac{K_{\mathrm{p}\_FO}}{\mathrm{s}\left(T_{1\_FO} s^{q_1} + T_{2\_FO} s^{q_2} + 1\right)}. \tag{17}$$

After substitution of relation 17 to equation 4, parameters q_1 q_2 K_{p_FO}, T_{1_FO} and T_{2_FO} were determined.

The tested pneumatic drive consisting of the actuator together with the control valve has the character of an integrating-type object with an oscillating element. To better reflect the physical aspect of the model, the description of the object was used by means of a non-integer differential calculus. Lambda and mi exponents that determine the derivative order have values close to integers, and reflect the nature of the tested pneumatic drive model being described in an effective manner.

After determining coefficients of the transfer function model, it takes the following form:

$$H(s)_{FO} = \frac{2.317}{\mathrm{s}\left(0.00208 s^{1.717} + 0.02287 s^{0.978} + 1\right)}. \tag{18}$$

In Fig. 5, three responses of the system are presented in the normalized scale: the measured one, simulated integer order, and simulated fractional-order, respectively.

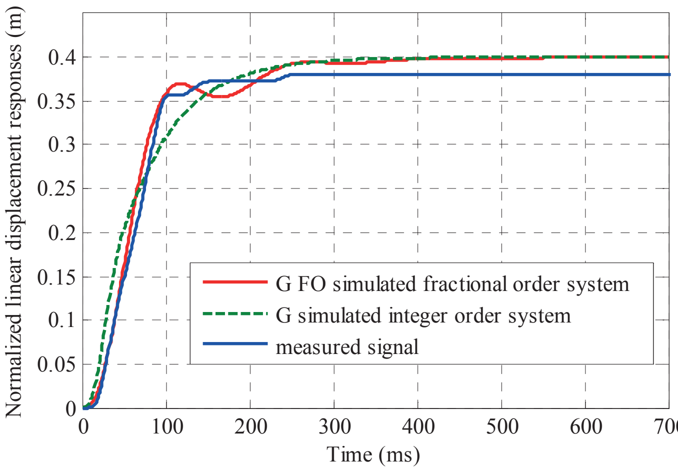

Fig. 5. Measured and simulated excitation steps

3. Controllers

As mentioned in the introduction, we can also find papers using the fractional order calculus in control theory, but such papers usually have a theoretical context. It should be noted that the number of works in which real applied plants and controllers of fractional order are analyzed remains very small.

The main reason for this situation is the difficulty with controller implementation and it is the result of the mathematical character of fractional operators, which are defined by convolution. It should be noted that transfer from mathematical form of the fractional order controller to a microcontroller system is very difficult.

3.1. Classic controller. In the first stage, a classic *PID* controller was tuned using quality integral criteria, and parameters K_p, K_i and K_d were calculated [11, 12, 18]. Coefficients were obtained based on integral quality criteria [12, 19, 20]:

$$\text{Integral square error} \int_0^t e^2(t)\mathrm{d}t$$

The controller has the following form:

$$C(s)_C = \frac{X(s)}{Y(s)} = K_p + K_i s^{-1} + K_d s, \tag{19}$$

where:

$$K_p = 6.786,\ K_i = 0.07022,\ K_d = 0.0216$$

and then

$$C(s)_C = \frac{X(s)}{Y(s)} = 6.786 + 0.07022 s^{-1} + 0.0216 s, \tag{20}$$

3.2. Fractional-order controllers. In the next step, the parameters $PI^{\lambda}D^{\mu}$ of the controller were determined. This means that a fractional order controller in the form of $PI^{\lambda}D^{\mu}$ was proposed. It can be generalized as the form of the *PID* controller with integral and differential terms of a fractional order with positive exponent λ, μ.

The transfer function of such type of controller in the Laplace domain take form [21].

$$C(s)_{CF} = \frac{X(s)}{Y(s)} = K_{pF} + K_{iF}s^{-\lambda} + K_{dF}s^{\mu}, \ (\lambda, \mu > 0) \quad (21)$$

where: K_{pF} is the proportional constant, K_{iF} is the integration constant and K_{dF} is the differentiation constant. Substituting $\lambda = 1$ and $\mu = 1$, we get a classic *PID* controller. However, if $\lambda = 0$ and $K_{pF} = 1$, we obtain a PD^{μ} controller, etc.

All *PID* controllers are a special case of the $PI^{\lambda}D^{\mu}$ controller. Therefore, the $PI^{\lambda}D^{\mu}$ controller has greater possibility of implementation.

3.3. $PI^{\lambda}D^{\mu}$ controller design and tuning. The fractional-order *PID* controller was first introduced by Podlubny in [22]. This generalized controller is called the $PI^{\lambda}D^{\mu}$ controller and has an integrator with order λ and a differentiator of order μ. Recent studies show that the fractional-order *PID* outperforms the classical *PID* [23–25]. Obviously, when taking $\lambda = \mu = 1$, the result is the classical integer-order *PID* controller. With more freedom in tuning the controller, the four-point *PID* diagram can now be seen as a *PID* controller plane, which is conveyed in Fig. 6.

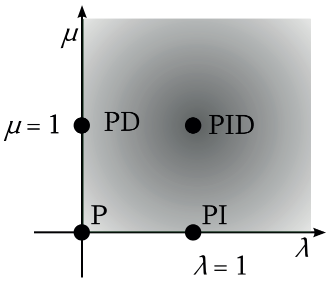

Fig. 6. $PI^{\lambda}D^{\mu}$ controller plane

In the subsequent step, the determined gain coefficients K_p, K_i and K_d were entered into the $PI^{\lambda}D^{\mu}$ controller and then coefficients $\lambda = 1$ and $\mu = 1$ were tuned in the Matlab optimization toolbox. The parameters of the FOC selection have been developed over the last ten years by many researchers [16, 22, 26].

Finally, the $C(s)_{FO}$ controller coefficients were obtained:

$$C(s)_{FO} = 7.609 + 29.365s^{-0.011} + 0.799s^{1.134}. \quad (22)$$

Figure 7 to 10 show the simulation results of plant $G(s)_{ob}$ described by the transfer function of integer order.

Simulations were performed for both the classic *PID* controller and the fractional order controller $PI^{\lambda}D^{\mu}$.

Simulations were done for typical excitation signals, the step, ramp and sinusoid multi-pulses position profiles.

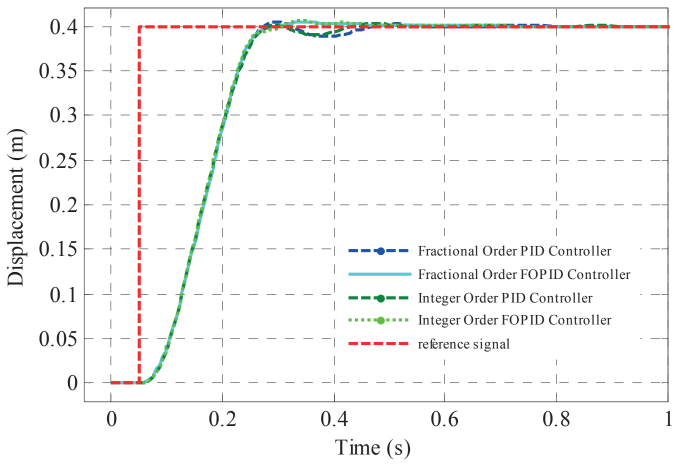

Fig. 7. System responses to step position profile

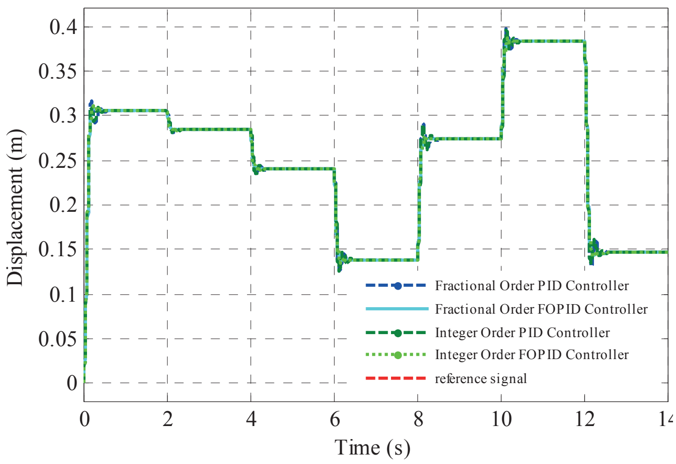

Fig. 8. System responses to multi-pulses position profile

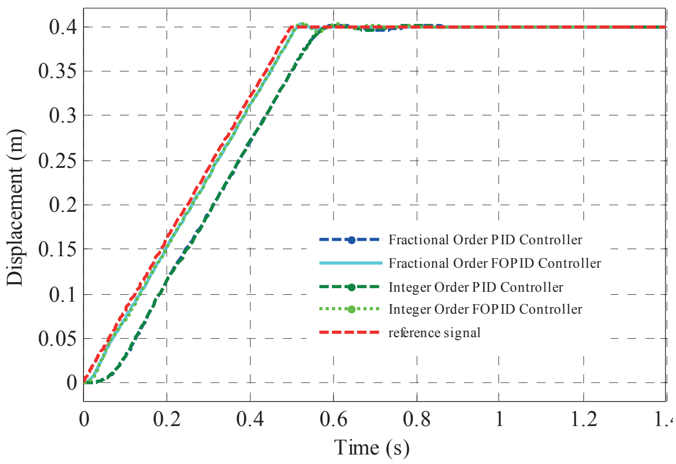

Fig. 9. System responses to ramp signal

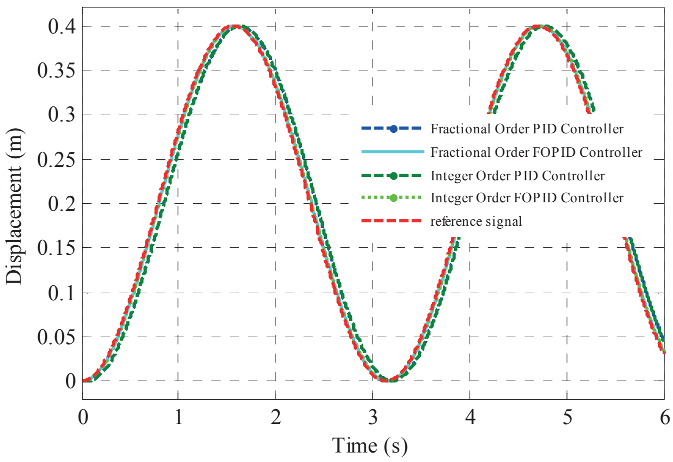

Fig. 10. System responses to sine wave signal

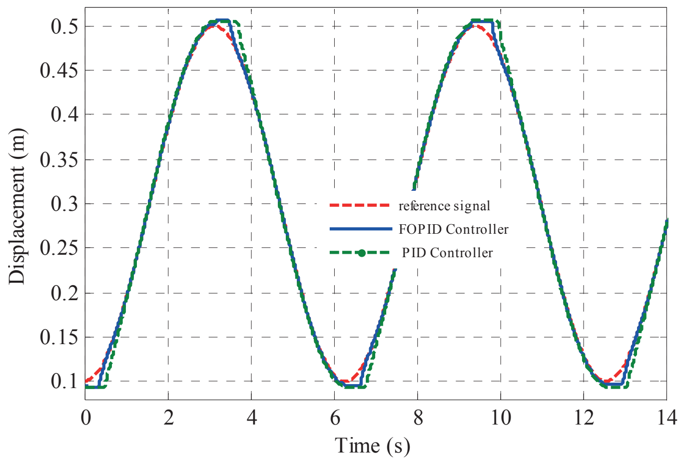

Fig. 13. System responses to sine wave signal

3.4. Experimental research. Figure 10 to 12 show the experiment results of plant $G(s)_{ob}$ described by the transfer function of integer order. Experiments were performed for both the classic *PID* controller and the fractional order controller $PI^{\lambda}D^{\mu}$.

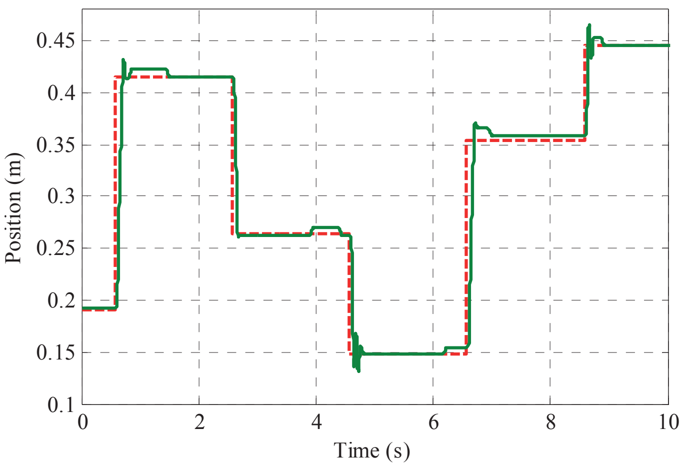

Fig. 11. System responses to multi-pulses position profile

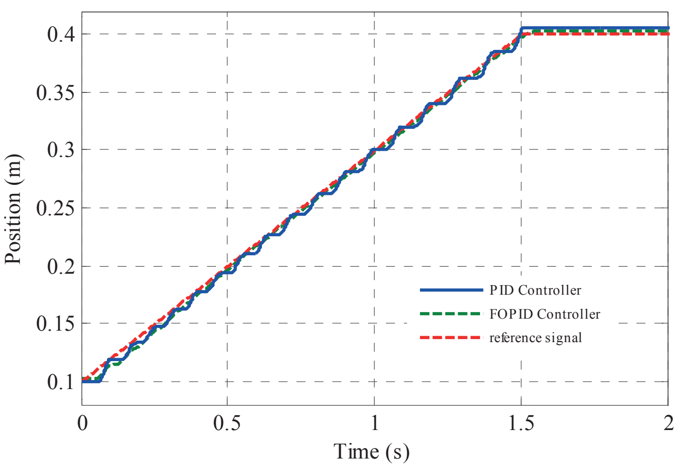

Fig. 12. System responses to ramp signal

Experiments were done for typical excitation c, the step, ramp and sinusoid multi-pulses position profiles.

Table 1 presents the integral quality criteria from the tests conducted.

Table 1
Integral quality criteria $ISE = \int_0^t e^2(t)\mathrm{d}t$

Simulation research

reference signal	Integer PID controller	Integer + FO PID controller	Fractional order PID controller	Fractional order FOPID controller	Time (s)
sine wave	0.00451	0.00016	0.00452	0.00016	14
step	0.01409	0.01407	0.01410	0.01408	1.4
ramp	0.00119	0.00005	0.00119	0.000045	1.4
multi step	0.01309	0.01286	0.01298	0.01275	14

Experimental research

reference signal	FOPID controller	PID controller	Time (s)
ramp	0.00005	0.00007	2
sine	0.00029	0.00142	14
multi step	0.00766	–	10

4. Conclusions

This paper presented a case study of fractional order feedback control of a pneumatic servo-drive. Based on the experimental and simulation tests performed, it can be noted that for the $PI^{\lambda}D^{\mu}$ type controller, the results of following up a set signal are better than for the classic *PID* controller. One of the cases in which both controllers do not meet the requirements is that of dynamic point-to-point movements. This is due to the fact of high friction forces and the stick-slip phenomenon.

In the future, we will conduct further research and describe a plant where exponents of the fractional order function will not be constant.

References

[1] C.-R. Rad and O. Hancu, An improved nonlinear modelling and identification methodology of a servo-pneumatic actuating system with complex internal design for high-accuracy motion control applications, *Simul. Model. Pract. Theory. 75* (2017) 29–47. doi:10.1016/j.simpat.2017.03.008.

[2] J. Zwierzchowski, Design type air engine Di Pietro, in: P. Dancova (Ed.), Exp. Fluid Mech. 2016 (EFM16), E D P SCIENCES, 17 Ave Du Hoggar Parc D Activites Coutaboeuf Bp 112, F-91944 Cedex A, France, 2017. doi:10.1051/epjconf/201714302149.

[3] A. Saleem, B. Taha, T. Tutunji, and A. Al-Qaisia, Identification and cascade control of servo-pneumatic system using Particle Swarm Optimization, *Simul. Model. Pract. Theory. 52* (2015) 164–179. doi:10.1016/j.simpat.2015.01.007.

[4] K. Khayati, P. Bigras, and L.-A. Dessaint, LuGre model-based friction compensation and positioning control for a pneumatic actuator using multi-objective output-feedback control via LMI optimization, *Mechatronics. 19* (2009) 535–547. doi:10.1016/j.mechatronics.2008.12.006.

[5] G.F. Bracha, Modeling a pneumatic cylinder with friction, in: V. Zolotarev, I and Radolf (Ed.), Eng. Mech. 2016, Acad Sci Czech Republic, Inst Thermomechanics, Dolejskova 5, Prague 8, 182 00, Czech Republic, 2016: pp. 90–93.

[6] P.A. Laski, Proportional valve with a piezoelectric actuator, in: EPJ Web Conf., 2017. doi:10.1051/epjconf/201714302064.

[7] J.E. Takosoglu, P.A. Laski, and S. Blasiak, Innovative modular pneumatic valve terminal with self-diagnosis, control and network communications, in: V. Fuis (Ed.), Eng. Mech. 2014, Acad Sci Czech Republic, Inst Thermomechanics, Dolejskova 5, Prague 8, 182 00, Czech Republic, 2014: pp. 644–647.

[8] D. Pietrala, The characteristics of a pneumatic muscle, in: P. Dancova (Ed.), Exp. Fluid Mech. 2016 (EFM16), E D P SCIENCES, 17 Ave Du Hoggar Parc D Activites Coutaboeuf Bp 112, F-91944 Cedex A, France, 2017. doi:10.1051/epjconf/201714302093.

[9] M.-K. Chang, J.-J. Liou, and M.-L. Chen, T–S fuzzy model-based tracking control of a one-dimensional manipulator actuated by pneumatic artificial muscles, *Control Eng. Pract. 19* (2011) 1442–1449. doi:10.1016/j.conengprac.2011.08.002.

[10] H.P.H. Anh and K.K. Ahn, Hybrid control of a pneumatic artificial muscle (PAM) robot arm using an inverse NARX fuzzy model, *Eng. Appl. Artif. Intell. 24* (2011) 697–716. doi:10.1016/j.engappai.2010.11.007.

[11] S.N. Syed Salim, M.F. Rahmat, A. 'Athif Mohd Faudzi, Z.H. Ismail, and N. Sunar, Position Control of Pneumatic Actuator Using Self-Regulation Nonlinear PID, *Math. Probl. Eng. 2014* (2014) 1–12. doi:10.1155/2014/957041.

[12] A. Blim, L. Jarecki, and S. Blonski, Modeling of pneumatic melt drawing of polypropylene super-thin fibers in the Laval nozzle, *Bull. Pol. Ac.: Tech.* 62 (2014). doi:10.2478/bpasts-2014–0005.

[13] C.A. Monje, Fractional-order systems and controls: Fundamentals and applications, Springer, London [u.a.], 2010.

[14] S. Blasiak, Time-fractional heat transfer equations in modeling of the non-contacting face seals, *Int. J. Heat Mass Transf. 100* (2016) 79–88. doi:10.1016/j.ijheatmasstransfer.2016.04.040.

[15] M. Sowa, A subinterval-based method for circuits with fractional order elements, *Bull. Pol. Ac.: Tech.* 62 (2014). doi:10.2478/bpasts-2014–0047.

[16] A. Tepljakov, Fractional-order Modeling and Control of Dynamic Systems, *Springer International Publishing, Cham,* 2017. doi:10.1007/978–3–319–52950–9.

[17] T. Marinov, N. Ramirez, and F. Santamaria, Fractional integration toolbox, *Fract. Calc. Appl. Anal. 16* (2013). doi:10.2478/s13540–013–0042–7.

[18] W. Kolaj, J. Mozaryn, and M. Syfert, PLC-PIDTuner: Application for PID Tuning with SIMATIC S7 PLC Controllers, in: 2016 21ST Int. Conf. METHODS Model. Autom. Robot., IEEE, 345 E 47TH ST, NEW YORK, NY 10017 USA, 2016: pp. 306–311.

[19] M. Viteckova and A. Vitecek, Simple Digital Controller Tuning, in: Petras, I and Podlubny, I and Kacur, J and Nawrocka, A and Sapinski, B (Ed.), Proc. 2013 14TH Int. Carpathian Control Conf., IEEE, 345 E 47TH ST, New York, Ny 10017 USA, 2013: pp. 428–431.

[20] T. Żabiński and L. Trybus, Tuning P-PI and PI-PI controllers for electrical servos, *Bull. Pol. Ac.: Tech. 58* (2010). doi:10.2478/v10175–010–0005–7.

[21] M. Blasiak and S. Blasiak, Application of fractional calculus in harmonic oscilator, in: Eng. Mech. 2017, Acad Sci Czech Republic, Inst Thermomechanics, Dolejskova 5, Prague 8, 182 00, Czech Republic, 2017: pp. 146–149.

[22] I. Podlubny, Fractional-order systems and PI/sup /spl lambda//D/sup /spl mu//-controllers, *IEEE Trans. Automat. Contr. 44* (1999) 208–214. doi:10.1109/9.739144.

[23] M. Zamani, M. Karimi-Ghartemani, N. Sadati, and M. Parniani, Design of a fractional order PID controller for an AVR using particle swarm optimization, *Control Eng. Pract. 17* (2009) 1380–1387. doi:10.1016/j.conengprac.2009.07.005.

[24] W. Mitkowski, J. Kacprzyk, J. Baranowski, eds., Advances in the Theory and Applications of Non-integer Order Systems, Springer International Publishing, Heidelberg, 2013. doi:10.1007/978–3–319–00933–9.

[25] A. Babiarz, A. Czornik, J. Klamka, M. Niezabitowski, eds., Theory and applications of non-integer order systems: 8th conference on non-integer order calculus and its applications, Zakopane, Poland, Springer, Cham, 2017.

[26] C.A. Monje, B.M. Vinagre, V. Feliu, and Y. Chen, Tuning and auto-tuning of fractional order controllers for industry applications, *Control Eng. Pract. 16* (2008) 798–812. doi:10.1016/j.conengprac.2007.08.006.